Graphical Abstract

Molecular Dynamics and Network Analysis Reveal the Contrasting Roles of Polar Solutes Within Organic Phase Amphiphile Aggregation

Biswajit Sadhu, Aurora E. Clark

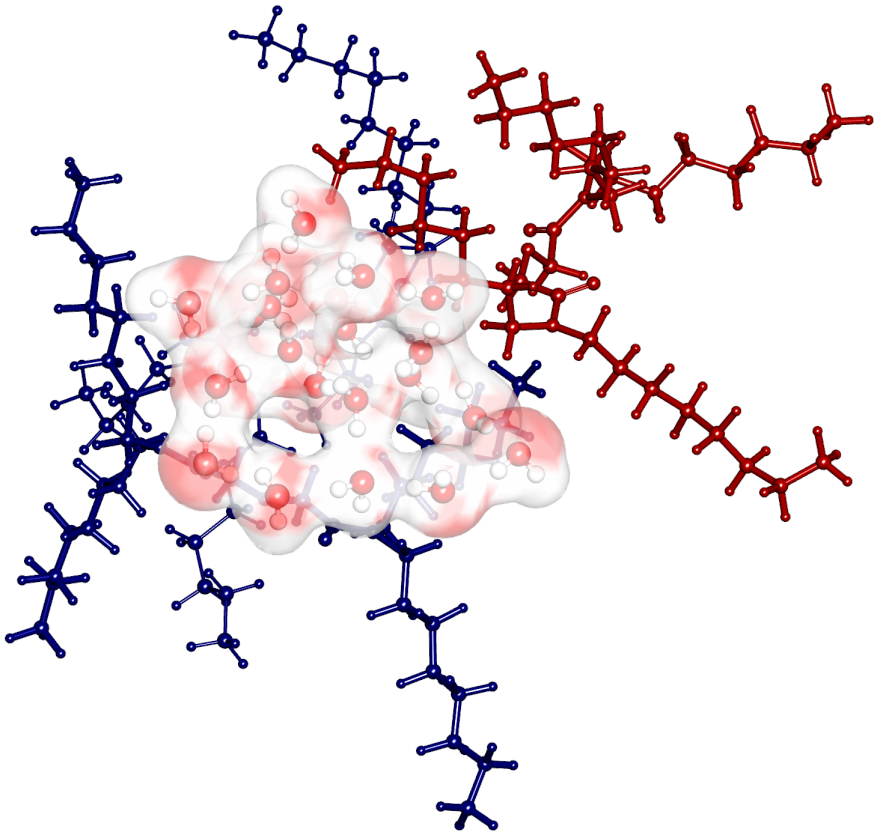

Highlights

Molecular Dynamics and Network Analysis Reveal the Contrasting Roles of Polar Solutes Within Organic Phase Amphiphile Aggregation

Biswajit Sadhu, Aurora E. Clark

- Concentration-dependent competition of hydrogen bonding among polar-solutes modulates the self-assembly of amphiphiles in non-polar media.
- Variations in hydrogen-bond donor and acceptor sites and hydrogen bond strength can lead to divergent self-assembly behavior under different conditions.
- Preferential self-solvation among H_2O leads to large water clusters that bridge amphiphile aggregates and support extended aggregation.
- Nitric acid disrupts H_2O hydrogen bonding and switches self-assembly from extended to local aggregation.

Molecular Dynamics and Network Analysis Reveal the Contrasting Roles of Polar Solutes Within Organic Phase Amphiphile Aggregation

Biswajit Sadhu[a,b], Aurora E. Clark[a,c,d]

[a] *Department of Chemistry, Washington State University, Pullman, 99164, WA, USA*
[b] *Health Physics Division, Health Safety Environment Group, Bhabha Atomic Research Centre, Mumbai, 400085, Maharashtra, India*
[c] *Voiland School of Chemical Engineering and Bioengineering, Washington State University, Pullman, 99164, WA, USA*
[d] *Pacific Northwest National Laboratory, Richland, 99354, WA, USA*

Abstract

Amphiphile self-assembly in non-polar media is often enhanced by polar co-solutes. This is observed within many biphasic separations processes, where amphiphiles mediate transport of water and acid into organic solution. A myriad of competitive intermolecular interactions have thus far prevented a fundamental understanding of the individual and dual role of these polar solutes upon amphiphile self-assembly in non-polar media. Toward this end, the current work employs classical molecular dynamics and intermolecular network analyses to deconstruct the individual affects of water and nitric acid upon the self-assembly of N,N,N′,N′-tetraoctyl-3-oxapentanediamide (TODGA), a prevalent amphiphile extractant used in metal ion separations. In the absence of acid, and at low water concentration, H_2O is found to promote local dimer and trimer formation of TODGA, however as $[H_2O]_{org}$ increases, preferential self-solvation leads to large $(H_2O)_n$ clusters that cause TODGA clusters to sorb to the $(H_2O)_n$ periphery and supports extended aggregation. Addition of HNO_3 to the humid solutions disrupts the water hydrogen bond network and inhibits the formation of large water clusters - thus preventing extended aggregation behavior and encouraging local aggregation. Prior experimental observations of enhanced TODGA self-assembly

Email addresses: bsadhu@barc.gov.in, biswajit.sadhu@wsu.edu (Biswajit Sadhu), auclark@wsu.edu (Aurora E. Clark)

under these conditions are attributed primarily to the role of water rather than co-extracted HNO_3, thus providing valuable new insight into the means by which extractant aggregation can be tuned within separations processes. The different roles of polar co-solutes, that derive from their individual hydrogen bonding capabilities and competitive interactions in the context of preferred solvation environments, is of fundamental importance amphiphile behavior in non-polar media.

Keywords: Amphiphile, self-assembly, liquid-liquid extraction, aggregation, graph theory, molecular dynamics, multicomponent solutions

---

1. Introduction

Amphiphile self-assembly is a ubiquitous process throughout polymer,[1, 2, 3] protein,[4] and catalysis[5] chemistry. The duality of amphiphile interactions with polar and non-polar solvents or co-solutes drives the formation of hierarchically organized structures like polymeric vesicles and micelles that are essential to drug delivery devices,[6, 7, 8] and also surface activity that supports their role as transporting extractants within the biphasic purification of complex mixtures (as in liquid-liquid extraction - LLE).[9, 10] Within LLE, amphiphilic extractants selectively partition specific solutes from the aqueous into the organic phase, however water and acids are often co-extracted, a feature that can enhance self-assembly and lead to a wide range of structures that influence separations efficiency (both in the distribution coefficients and solute selectivity).[11] Self-assembly in such organic solutions presents an interesting scenario, where competition of intermolecular interactions amongst scarce donor and acceptor groups have the potential to strongly influence aggregate size, composition, and topology. Indeed, at high concentrations, extractant aggregatation can lead to undesirable phase splitting,[12] but at moderate concentrations an increase in extraction efficiency can be observed - supposedly because the aggregates themselves are better extractants than the individual extractant-solute (or metal-ligand, ML) complexes.[13] The organizational structure of aggregates, their diversity in volume, stoichiometry, and associated micro-structural features have been proposed to influence individual solute transport events and if multiple extractants are employed synergism may be observed.[14, 15]

Presumably, features like the dipole moment or hydrogen bonding of polar co-solutes influence amphiphile self-assembly, as would be inferred from extensive studies in aqueous solutions.[16, 17] Yet in many cases, identifying the individual role of a specific co-solute in non-polar media is a challenge that has yet to be overcome. In the case of LLE, the co-extraction of both water and acid is highly varied, as is the impact upon extractant aggregation. The water concentration in the organic phase, $[H_2O]_{org}$, is not only dependent on the characteristics of the amphiphile extractant but also on the specific acid.[18] While HNO_3 increases $[H_2O]_{org}$, other strong acids like HCl do not.[18] At the same time, the acid extraction in the organic phase depends upon its individual interactions with both metal-extractant complexes and free extractant amphiphile molecules.[19] These dependencies often ensure the simultaneous presence of water and acid in the organic medium

albeit at varying concentration.[20, 21] Given this, amphiphile self-assembly in LLE systems has been attributed, somewhat vaguely, to complex coupled interactions within an amphiphile–water–acid network (as supported by FTIR[22]).

Within this construct, we *hypothesize* that the organic solution (relative to an aqueous solution) supports enhanced competition amongst the varying hydrogen bond capabilities of polar solutes that tune amphiphile self-assembly in the context of the locality of the amphiphile interactions. Molecular dynamics methods provide a well-established methodology to test this hypothesis, particularly when advanced sub-ensemble analsysis techniques are employed to reveal the correlating relationships of hydrogen bond characteristics and aggregate formation. A well-known LLE system is used as a platform to learn about how hydrogen bonding influences the size and composition of the resulting aggregates and also the patterns of intermolecular interactions that govern their morphology in the context of concentration dependent HB and solvation competition. Specifically, N,N,N′,N′-tetraoctyl-3-oxapentanediamide (TODGA) is a representative diglycolamide amphiphile, whose behavior in *n*-dodecane is relevant to the separation and purification of critical elements, actinides and lanthanides within the nuclear fuel cycle (notably the Actinide Lanthanide SEParation Process (ALSEP)).[23, 24] Further, this amphiphile can exhibit phase splitting behavior at moderate acid concentration.[25] The acid driven aggregation of TODGA, even in the absence of metal ions, has been experimentally studied using small-angle neutron scattering (SANS) and vapor-pressure osmometry (VPO).[13, 26, 27] Within this work, benchmarked simulation is used to precisely control the polar co-solute concentration in the organic phase, while analysis of the hydrogen bond network identifies the correlating relationships of solute hydrogen bonding and amphiphile aggregation.

The available experimental data and diverse aggregation behavior of TODGA is ideal for developing a platform of basic insight into the competition amongst varying hydrogen bond (HB) capabilities of polar solutes upon amphiphile aggregation in non-polar media. Simulations are used here to show that H_2O and HNO_3 have different mechanistic roles that facilitate amphiphile self-assembly - where clear differentiation is observed upon the resulting aggregate size distribution, composition, and morphology. As $[H_2O]_{org}$ is increased the dual hydrogen bond accepting and donating capabilities cause a transition from H_2O acting as an individual bridging constituent between TODGA molecules, to preferential self-solvation that causes larger water

clusters to be formed whose surfaces bring together TODGA clusters that form extended aggregate assemblies. Addition of HNO_3 to the humid organic solutions disturbs the preferential self-solvation of water by rearranging its HB network to participate in the multiple HB acceptor sites of HNO_3. This in turn inhibits the formation of large water clusters that support TODGA aggregate–aggregate merging. *Despite the prevalent assumption within the experimental literature that HNO_3 is generally responsible for the growth of TODGA assemblies in upon coextraction of H_2O and HNO_3, this work instead proposes that it is the underlying role of water that contributes to the observed aggregation phenomena.* We anticipate that these mechanistic insights, and the role of HB competition amongst polar co-solutes, will help achieve better control over amphiphile self-assembly across length-scales in non-polar media and may assist process layouts that leverage such aggregation in liquid-liquid extraction and other industrial applications.

2. Materials and Methods

2.1. Simulation Protocol

System Composition Table 1 presents the composition of all simulated systems, with different conditions labelled **A - C**. System **A** corresponds to 0.1 M TODGA dissolved in *n*-dodecane, and is based on the experimental critical micelle concentration (CMC) of TODGA at 2 M $[HNO_3]_aq$ and 25°C.[26, 27] The **B**-series of systems introduce water to TODGA/*n*-dodecane, where the water concentration is gradually increased from **B1** (0.02 M) to **B2** (0.05 M) to **B3** (0.2 M H_2O). In the **C**-series, nitric acid is introduced to water-containing conditions. The **C1** and **C2** systems correspond to prior experimental studies that have 0.02 M and 0.05 M HNO_3[26, 13, 27] and the same water content as **B1** and **B2**, respectively. The **C3** - **C5** series have the 0.20 M H_2O content of **B3** and varying $[HNO_3]$ up to 0.15 M.

Force Field Implementation The interactions of *n*-dodecane were taken from [28], while the force field of TODGA was generated by the Generalized AMBER Force Field (GAFF2)[29] parametrization using the geometry-optimized structure of TODGA using density functional theory (DFT) with the B3LYP[30, 31] functional and 6-31G* basis set[32]. The restrained electrostatic potential (RESP) approach was employed to derive the partial charges. This protocol follows a similar approach to that of [33], where AMBER force field parameters with RESP-fitted charges were employed to investigate the complexation of Ln^{3+} and $UO_2{}^{2+}$ with a tetra-methyl DGA

Table 1: Compositions of simulated systems

Conditions	TODGA (M)[a]	Water (M)[a]	Nitric Acid (M)[a]
A	0.10 [60]	-	-
B1	0.10 [60]	0.02 [12]	-
B2	0.10 [60]	0.05 [30]	-
B3	0.10 [60]	0.20 [120]	-
C1[b]	0.10 [60]	0.02 [12]	0.01 [6]
C2[c]	0.10 [60]	0.05 [30]	0.05 [30]
C3	0.10 [60]	0.20 [120]	0.01 [6]
C4	0.10 [60]	0.20 [120]	0.05 [30]
C5	0.10 [60]	0.20 [120]	0.15 [90]

[a]Values in bracket correspond to the number of molecules present in the simulation. [b]Experimental conditions of Nave et al.[26] [c]Experimental conditions of Yaita et al.[13]

extractant (TMDGA). As part of the benchmarking process we note that the employed parameters reproduce the correct density of 0.1 M TODGA in *n*-dodecane as (predicted to be 0.788 gL^{-1} relative to the experimental value of 0.759 gL^{-1}[34]), and measured diffusion coefficient[35] (see Results section and Supporting Information). The dodecane/water interfacial tension, using the TIP3P water model[36] is also reproduced for the sake of benchmarking (with a value of 51.2 mNm^{-1} being obtained relative to the experimental value of 50.74 $\pm$ 0.08 mNm^{-1}[37]). In the single-phase system that is the focus of this work, the TIP3P water model[36] was used along with the HNO_3 parameters of [38] which uses the molecular (undissociated) form that is congruent with experimental IR[39] and *ab-initio* theoretical predictions.[40, 18] Additional details regarding the force field parameters are provided in the Supporting Information (see Figure S1, Table S3-S4).

Molecular Dynamics Simulations Although the final system compositions are reported in Table 1, benchmarking of the computational protocol began with examining the system size dependence for the **C4** condition. Two different box sizes were constructed, the first 15 $\times$ 15 $\times$ 15 nm and the second 10 $\times$ 10 $\times$ 10 nm. The initial system configurations were generated using Packmol[41] by distributing all molecules randomly in the cubic box. The volume of diluent was corrected considering the equivalent volume of replacement of added TODGA, H_2O and HNO_3. The simulation box constitutes a

representation of the organic phase and no interface was generated during equilibration. Subsequent molecular dynamics simulations were performed using GROMACS 2019.4[42] using one of two different equilibration procedures. In the first equilibration procedure, the two simulation box sizes were first energy-minimized using steepest descent, then subjected to 40 ns of NPT molecular dynamics at 300 K and 1 bar using the Berendsen pressure-coupling[43] with a 2 fs time step. This was followed by a further 40 ns equilibration in NVT with Nosé-Hoover thermostat[44] (time constant(τ) = 0.4 ps). In the second equilibration procedure 20 ns of NPT and 20 ns of NVT were used. This was followed by 100 ns of a production run in NVT for analysis of the equilibrium properties at a sampling interval of 10 ps. A cut off of 15 Å was applied to account for the short-range electrostatic and van der Waals interactions. The particle mesh Ewald method[45] was employed for the long-range electrostatics interaction. The LINCS algorithm[46] was implemented to constrain the bond between H-atom and a bound heavy atom at its equilibrium length. As demonstrated in Figure S2, the RDF between ethereal oxygen atoms for the two box sizes and equilibration procedures are nearly identical. Thus, to maintain reasonable computational cost only the $10 \times 10 \times 10$ nm simulation box was employed for all other system compositions, where equilibration consisted of the 20 ns of NPT and 20 ns of NVT followed by 100 ns of production run for all analyses.

2.2. Analysis Methods

Construction of Intermolecular Networks of Interactions Undirected, unweighted graphs (networks) were generated for each frame of the trajectory by considering each individual molecule as a vertex (or node), and an edge existing between nodes if certain distance criteria are satisfied. Graphs were generated from the 100 ns production trajectories at a sampling interval of 100 ps. The ChemNetworks[47] software was employed for graph construction, as this accounts for periodic boundary conditions and contains several graph correction and analysis features (*vide infra*). Further analysis of the different graph-based descriptors were carried out using the NetworkX python package.[48]

Clusters (or aggregates) are defined as the components that are disconnected from the total network, where the composition of the cluster classifies the aggregate as either "homogeneous" (all nodes are the same type of molecule) or "heterogeneous" (nodes representing different molecular types).

Note that some heterogeneous clusters can be composed of smaller homogeneous domains. Based on the system composition, three homogeneous aggregates can be formed, comprised solely of TODGA, water or nitric acid, and four heterogeneous aggregates may be formed, consisting of TODGA-H_2O, TODGA-HNO_3, H_2O-HNO_3 and TODGA-H_2O-HNO_3. The cluster size is the total number of nodes within a component. Identifying the appropriate criterion for defining edges of interactions is a challenging task that requires significant consideration. A common practice is to obtain a distance-based cut-off upon the radial distribution function (RDF) between appropriate particle pairs.[49, 50] In the case of amphiphiles like TODGA a weak dipole-dipole interaction drives association that can be manifested in different pair-wise particle-particle correlations. Stronger, directed interactions - as in hydrogen bonding - support more straightforward edge definitions. Further, it is important to recognize that a rigid geometric criterion can introduce artifacts into the graph structure due to thermal oscillations around the cutoff criterion and these features must be corrected for (*vide infra*).

TODGA-TODGA Edge Definitions. TODGA is a large molecule, with an end-to-end distance above 24 Å; see Figure S3. Several different geometric criteria were examined to define TODGA-TODGA interactions, based upon potential hydrophilic interactions mediated by the TODGA core ethereal and carbonyl O-atoms, and steric and hydrophobic interactions associated with the four *n*-octyl chains. Three different geometric cut-off criteria (labelled I-III) were examined for solution conditions **C1** and **C2** (Table S7, Supporting information) where there exists experimental data regarding the preferred TODGA oligomeric states.[26, 13, 27]. Although detailed comparisons are provided within the Supplementary Information, the best agreement with experiments for the geometric criterion was obtained for criterion III (see Figure S4) which imposes a distance cutoff between inter-TODGA ethereal-ethereal O-atoms of 12 Å and a minimum tail-tail proximity of 7.5 Å (see Figure S3). A dynamics-based correction scheme proposed by Ozkanlar et al.[51] was employed with these cut-off values to help remove additional artifacts created by rigid cutoff parameters (referred as criterion III-corr in Supporting Information).

Definitions of Hydrogen Bonding. Several different types of hydrogen bonding interactions are possible among the polar solutes within different system compositions under study, including: H_2O...H_2O, H_2O...HNO_3 (water donating), O_3NH...OH_2 (nitric acid donating). Amongst water and nitric

acid, a distance cutoff of 2.5 Å was set between donor(H)-acceptor(O) for identifying hydrogen bond interactions. Further, for HBs among H_2O, an additional angle based cutoff criterion (less than 30° for ∠O-H...O) was imposed along with the distance threshold.[51] For HB interactions involving TODGA (i.e., H_2O...TODGA (water donating), O_3NH...TODGA (nitric acid donating)), a O...O distance cutoff of 3.8 Å was employed based on the first minimum of corresponding RDF profiles (see Figure S5).

Local vs. Extended Aggregation To learn more about the formation and growth of aggregates, as well as the changes to their the change network topology, two classes of clustering are delineated based upon the nature of the interactions that promote the aggregation process: 1) local aggregation and 2) extended aggregation. Local aggregation is characterized by a cluster that is dominated by TODGA nodes that have an edge irrespective of whether any H_2O or HNO_3 are present. In contrast, extended aggregation occurs when one or more homogeneous TODGA clusters are connected to a homogeneous water cluster, but where each TODGA cluster is distance-separated (having no edge) from the others. In other words, in the extended aggregation, water clusters link otherwise separated TODGA cluster(s) and in this manner TODGA clusters are connected through non-local interactions. The same definitions are applicable to HNO_3-containing cluster systems. Figure S6 illustrates the potential cluster compositions and their associated definitions.

Eccentricity Distribution Within Clusters. To evaluate the connectivity within the homo- and heterogeneous clusters, we computed the eccentricity distribution of all nodes using NetworkX.[48] Within the formalism of graph theory, the eccentricity (e_v) of a node is defined as the maximum graph-distance between the node with all other nodes present within the network.

$$e_v = max\{d(v,u), u \in \ v(G)\} \tag{1}$$

Here, $d(v,u)$ is the graph-distance between u and v node within graph G. The maximum eccentricity is the diameter of the graph.[52] Thus, the distribution of this parameter with respect to all nodes reflects the span and connectivity of the network. Nodes with higher eccentricities indicate their participation within a cluster that has longer pathways, while a minimum eccentricity value of 1 arises when the node is directly connected to all the other nodes within the network (occurring only in small clusters). An illustration of eccentricity distributions for several different graph topologies is illustrated in Figure S7.

3. Results and discussion

In the absence of a polar solute, TODGA molecules interact via weak electrostatic dipole-dipole forces. Experimentally, a dynamic equilibrium between a monomer and dimer is observed at a minimal concentration of H_2O and acid.[13, 27] This behavior is reproduced within solution **A**, where over 53 % of all TODGA remain in a monomeric state, 23 % in a dimer and 14 % in a trimer, while population of other higher oligomers remain < 10 % (see Figure 1) . Moving forward, we now consider solution **B** conditions, so as to rigorously understand the role of water upon aggregation, followed by the **C** solutions - where the perturbative role of HNO_3 is identified.

3.1. Concentration Dependent Aggregation Switching by Water

Although only 9 % of all TODGA participate in $(TODGA)_m(H_2O)_n$ clusters with $m > 3$ at 0.02 M H_2O, the growth of larger clusters is appreciable as water content is increased. At 0.05 M H_2O, 27 % of TODGA reside in clusters with $m > 3$ and at 0.2 M H_2O 34 % of TODGA exist in large clusters (Figure 1, Figure S8). These clusters are almost entirely heterogeneous in composition $(TODGA)_m(H_2O)_n$ and a significant decrease in the TODGA diffusion coefficient is observed (see Table S8, Supporting information). A non-linear, but positive, correlation is observed with respect to the water content within the heterogeneous clusters and the total cluster size (see Figure S9 and S10, Supporting information). Interestingly, the short-range TODGA-TODGA, TODGA-water and water-water nonbonded interaction energies (see Figure S11) as a function of $[H_2O]$ in the organic phase further indicate that the increase in water content has a noticeable *indirect* stabilizing effect on TODGA-TODGA interaction.

To elucidate whether water is serving to enhance local or extended aggregation, we begin by studying the distribution of H_2O in three different zones around individual TODGA molecules (see Table 2). The zones are defined based upon distances from the TODGA carbonyl and ethereal O-atoms using the *around* selection feature of the MDAnalysis toolkit.[53] Zone 1 is defined by a distance 0 - 0.38 nm, Zone 2 0.38 - 1 nm and Zone 3 > 1 nm. These results indicate that with increasing water in the organic media, the population of H_2O in Zone 2 (the 2^{nd} and 3^{rd} solvation shells of TODGA) increases more rapidly than in Zone 1 (the 1^{st} solvation shell). This complements the modest increase in hydrogen bonding between H_2O and TODGA

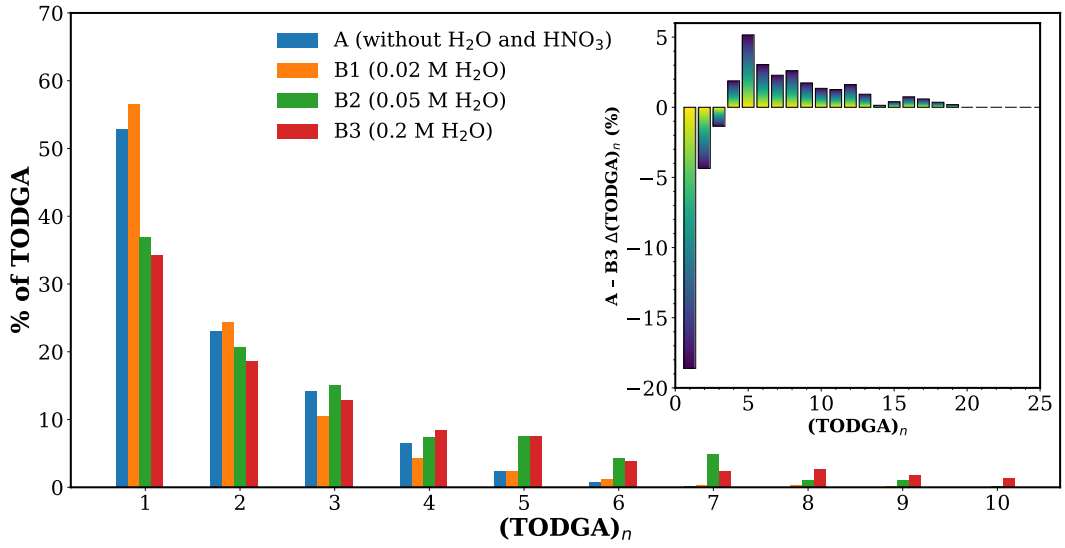

Figure 1: Cluster distribution with the increase of water concentration: Percentage of TODGA are plotted against the cluster size. The inset plot shows the relative change in the percentage of clusters against the cluster size from system A to B3.

versus a much sharper H_2O...H_2O HB increase as we traverse **B1** to **B2** to **B3** conditions (see Table 2).

The propensity for two different cluster configurations was then examined:

1. TODGA clusters that are solvated by separated water clusters (labelled "water-extractant-water" or "W-E-W"). In this type of arrangement TODGA molecules have direct interactions with each other and are connected components of the cluster subgraph. Thus W-E-W is considered local aggregation because of the locality of the TODGA-TODGA interactions.
2. Water clusters that link separated TODGA clusters (labelled "extractant-water-extractant" or "E-W-E"). These instances represent extended aggregation where TODGA interact through the HB network of water.

The distribution of E-W-E and W-E-W heterogeneous clusters is presented in Figure 2, as represented by the formation matrix whose rows and columns are the size of the terminal homogeneous sub-clusters while the inset presents the size distribution of the central (bridging) sub-cluster. In general, there is a predominance of W-E-W cluster configurations however

Table 2: (Top) Average number of hydrogen bonds (with standard deviation) among TODGA, H_2O and HNO_3. (Bottom) Percent distribution of water and nitric acid around TODGA O-atoms (out of all H_2O or HNO_3 present in the system). Three zones are defined based on the distance from the carbonyl and ethereal O-atoms; Zone 1: 0 - 0.38 nm, Zone 2: 0.38 - 1 nm, and Zone 3: >1 nm.

Conditions	Hydrogen Bonds			
	$H_2O...H_2O^a$	$TODGA...H_2O^b$	$H_2O...HNO_3^a$	$TODGA...HNO_3^b$
B1	0.21±0.08	0.14±0.03	-	-
B2	0.47±0.10	0.33±0.05	-	-
B3	1.22±0.05	0.46±0.06	-	-
C3	1.12±0.05	0.58±0.07	0.06±0.01	0.07±0.01
C4	1.02±0.04	1.02±0.08	0.24±0.02	0.21±0.01
C3	0.69±0.05	1.33±0.10	0.70±0.05	0.28±0.03

Conditions	Percent of Water			Percent of Nitric Acid		
	Zone 1	Zone 2	Zone 3	Zone 1	Zone 2	Zone 3
B1	77.09	17.73	5.17	-	-	-
B2	68.52	29.10	2.36	-	-	-
B3	38.83	59.56	1.60	-	-	-
C3	42.99	52.77	4.22	19.86	79.38	0.74
C4	53.02	45.79	1.18	50.16	48.74	1.09
C5	62.23	35.53	2.24	42.61	54.48	2.91

[a] Values indicate the average number of hydrogen bonds per H_2O. [b]Values correspond to the average number of hydrogen bonds per TODGA.

the frequency of E-W-E increases with increasing water concentration (see Figure S12, Supporting Information). Smaller $(H_2O)_n$ clusters are correlated with the W-E-W cluster configurations, whereas large water clusters are correlated with the E-W-E. As the total water content is increased the relative percent of E-W-E clusters increases from 0.6 % at 0.02 M H_2O (B1) to 2.0 % at 0.05 M H_2O (B2) to 18.5 % at 0.2 M H_2O (B3).

The topological properties of the network of intermolecular interactions provide new insight into the way in which different subgraphs within the E-W-E and W-E-W clusters interact. The eccentricity distribution of the molecular nodes (Eqn. 1) is presented in in Figure 3, and represents the maximum graph-distance between the node with all other nodes present within the network. Being a node-specific property, the distribution of eccentricities reflects the internal connectivity as well as the span of network. For TODGA-water mixed-aggregates, the shift towards higher eccentricities is substantial as we traverse from low concentration to high water concentration. This would be anticipated for the growth of the water cluster hydrogen bond network and its interactions with the TODGA clusters that it links together. In combination, these data support a role for water of acting as driving force behind local aggregation at low water content within the organic phase and that as the water content increases, competition emerges for the preferential solvation of H_2O with itself over solvation of TODGA. When larger water clusters are formed, they enable extended aggregation behavior within the solution where the total cluster size is further significantly larger than with the W-E-W configuration (Figure S13, Supporting information).

3.2. Nitric Acid Inhibits Extended Aggregation

In prior experimental studies[12, 54, 26], it is reported that an increase in $[HNO_3]_{aq}$ leads to growth of aggregate size within the organic phase. An increase in the stickness parameter required to fit SAXS data[54] also supports enhanced inter-aggregate interaction at higher aqueous acidities. However, it is difficult to interpret whether such effects derive solely from an increased $[HNO_3]_{org}$, as extracted acid may potentially form protonated solvates, for example of the form "extractant...$(HNO_3)_x$". Other hypotheses could easily be generated because as the $[HNO_3]_{org}$ increases - so too does $[H_2O]_{org}$. This introduces competitive or synergistic interactions as a result of the differing hydrogen bond capabilities of these two polar solutes.

The **B3** solution condition (0.2 M H_2O) was used as the basis for investigating the impact of HNO_3 on the aggregation of TODGA, where the

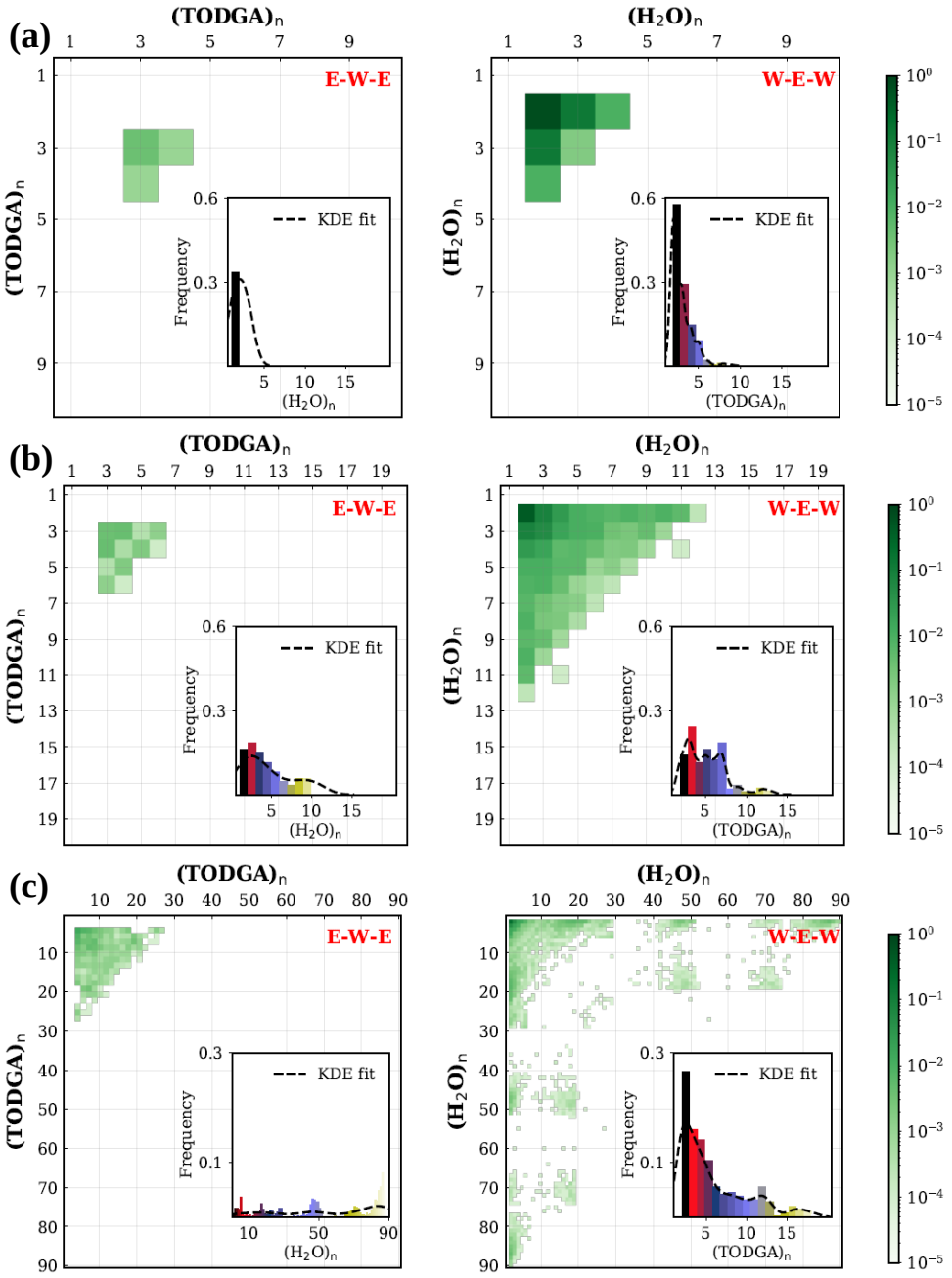

Figure 2: The growth of Extractant-Water-Extractant (E-W-E) mixed-aggregates where water bridges the TODGA clusters and Water-Extractant-Water (W-E-W) mixed-aggregates where TODGA bridges the water clusters for (a) B1 (top), B2 (middle) and B3 (bottom) solution conditions. The color bar is in logarithmic scale and indicate the normalized proportion of the total occurrences of E-W-E and W-E-W mixed-aggregates as function of the cluster sizes. The inset box within the plots shows the normalized frequency distribution of occurrences (Y axis) of the bridging constituents (left panel: water; right panel: TODGA) with respect to their cluster size (X axis). The shape of the distribution in the inset box is obtained using gaussian kernel density estimate (KDE).

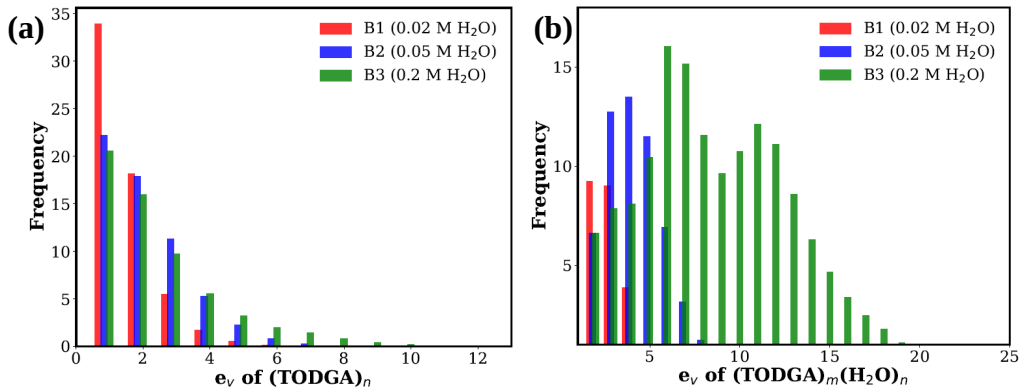

Figure 3: a) Distribution of eccentricities (e_v) associated with the TODGA clusters for B1, B2 and B3 system. b) Distribution of (e_v) associated with the TODGA-Water network for B1, B2 and B3 system. Frequency quantifies the total number of instances of e_v for all the molecules of associated aggregate and mized-aggregate type.

acid concentration is systematically increased from 0.01 M (forming the **C3** solution) to 0.05 M (**C4**) to 0.15 M (**C5**). Perhaps unsurprisingly, the single HB donor site of HNO_3 limits the ability of nitric acid form homogeneous aggregates and over 90 % of HNO_3 are observed to remain in a monomeric form (with no HB to other HNO_3). The molecular form of nitric acid has three HB acceptor sites and one donor site, which introduce significant competition for hydrogen bonding amongst the two HB acceptor and donor sites of H_2O. Analysis of the pair-wise interaction energies suggests an increasing stabilization of the HNO_3...H_2O interaction at the expense of destabilizing H_2O...H_2O interactions as $[HNO_3]_{org}$ increases (see Figure S14). As shown in Figure S15, introduction of HNO_3 also significantly perturbs the water clustering process where hydrogen bonding of H_2O and HNO_3 restricts the formation of water clusters over the size of ca. 30 within the **C5** solution. This is well-supported by the subsequent increase in solvent accessible surface area (SASA) per water molecule upon increasing acid concentration (Table S9, Supporting information). In-depth analysis on the inter-connectivity of the HNO_3...H_2O HB network suggests that with increasing concentration, HNO_3 participates in forming mixed aggregates of the form N-W-N (nitric acid-water-nitric acid) and W-N-W (water-nitric acid-water) with substantial preference for former (see Figure S16 and S17, Supporting Information). As a result, the presence of HNO_3 reduces the hydrogen bond network connectivity among H_2O and shortens the associated network length. The eccen-

tricity distributions of the hydrogen bond network of water clusters reflects a gradual reduction of graph distance between H_2O with increasing [HNO_3]. Concomitantly, there is a decreasing trend of hydrogen bonds between H_2O and an increase in the propensity of H_2O to solvate more TODGA molecules (growth in the average number of HBs between TODGA and H_2O shown in Table 2).

These data complement the observed changes to distribution of H_2O and HNO_3 around TODGA in various zones as [HNO_3] is increased. Specifically, the percentage of H_2O around TODGA in its 1^{st} solvation shell (Zone 1) increases whereas less waters partition within Zone 2 (see Table 2). At low [HNO_3] (0.01 M; **C3**), $>$ 80 % of HNO_3 remain in the Zone 2 while a significantly higher percentage migrate into the 1^{st} solvation shell of TODGA as the total nitric acid concentration is increased. Thus, there are enhanced interactions between both polar solutes and the hydrophilic core of TODGA as acid is added to the solution. The disruption in the water HB network by nitric acid has a direct impact over the cluster size distribution of TODGA and on the TODGA-water mixed-aggregates (Figure S18 and S19, Supporting information). Specifically, reducing the size of water clusters severely inhibits the formation of TODGA clusters that are linked by those water clusters as shown in Figure S15 (Supporting information). The size of the TODGA-water and TODGA-water-nitric acid mixed aggregates (see Figure 5) remains restricted due to the smaller core of water-nitric acid mixed-aggregates. Further, contrary to the case of water without acid, there is a decrease in the formation of E-W-E type of mixed-aggregates with increasing acid concentration (Figure 4 and Figure S12). The distribution of eccentricities of W-E-W and E-W-E aggregates also demonstrates a reduction of network length, suggesting that in the presence of water, nitric acid reduces the inter-connectivity among the mixed-aggregates (see Figure 6).

These predicted trends are somewhat counter-intuitive to the implied role of nitric acid within the experimental literature. Although, it has been perceived in several experiments[12, 54, 26] that increase in $[HNO_3]_{aq}$ leads to better amphiphile aggregation, it is important to emphasize that the aqueous acidity increases both the concentration of $[H_2O]_{\text{org}}$ and $[HNO_3]_{org}$.[18] This work demonstrates that H_2O supports both local and extended aggregation as its concentration in the organic phase increases, while the competitive hydrogen bond interactions with nitric acid decrease extended aggregation. Thus, we propose that the increase in the size of amphiphile aggregates observed in prior experiments likely derives from the enhanced concentration of

water (caused by coextraction with HNO_3) rather than the role of the acid upon self-assembly. Undoubtedly, the concentration of water in the organic phase is crucial to tune the degree of local and extended aggregation events involving nitric acid. A comparison of the **B1** and **C1** systems alongside the **B2** and **C2** systems provide further intuition about the dependency between nitric acid concentration and the extent of aggregation. The small quantity of acid that present in **C1** (0.02 M water and 0.01 M acid) relative to **B1** (0.02 M water) does not appreciably perturb the small existing water network. The dispersed H_2O and HNO_3 solvate TODGA molecules without little interaction amongst themselves. Indeed the size of TODGA clusters from **B1** to **C1** is increased by the individual bridging of the isolated polar solutes (see Figure S20, Supporting Information). Increasing the water and acid content to (i.e., **C2** (0.05 M water and 0.05 M acid); relative to **B2** (0.05 M water) creates competition between H_2O...H_2O hydrogen bonding and H_2O...HNO_3, and instead of the growth of large water clusters observed in the absence of nitric acid, the relative size of the TODGA clusters is restricted (see Figure S20, Supporting Information).

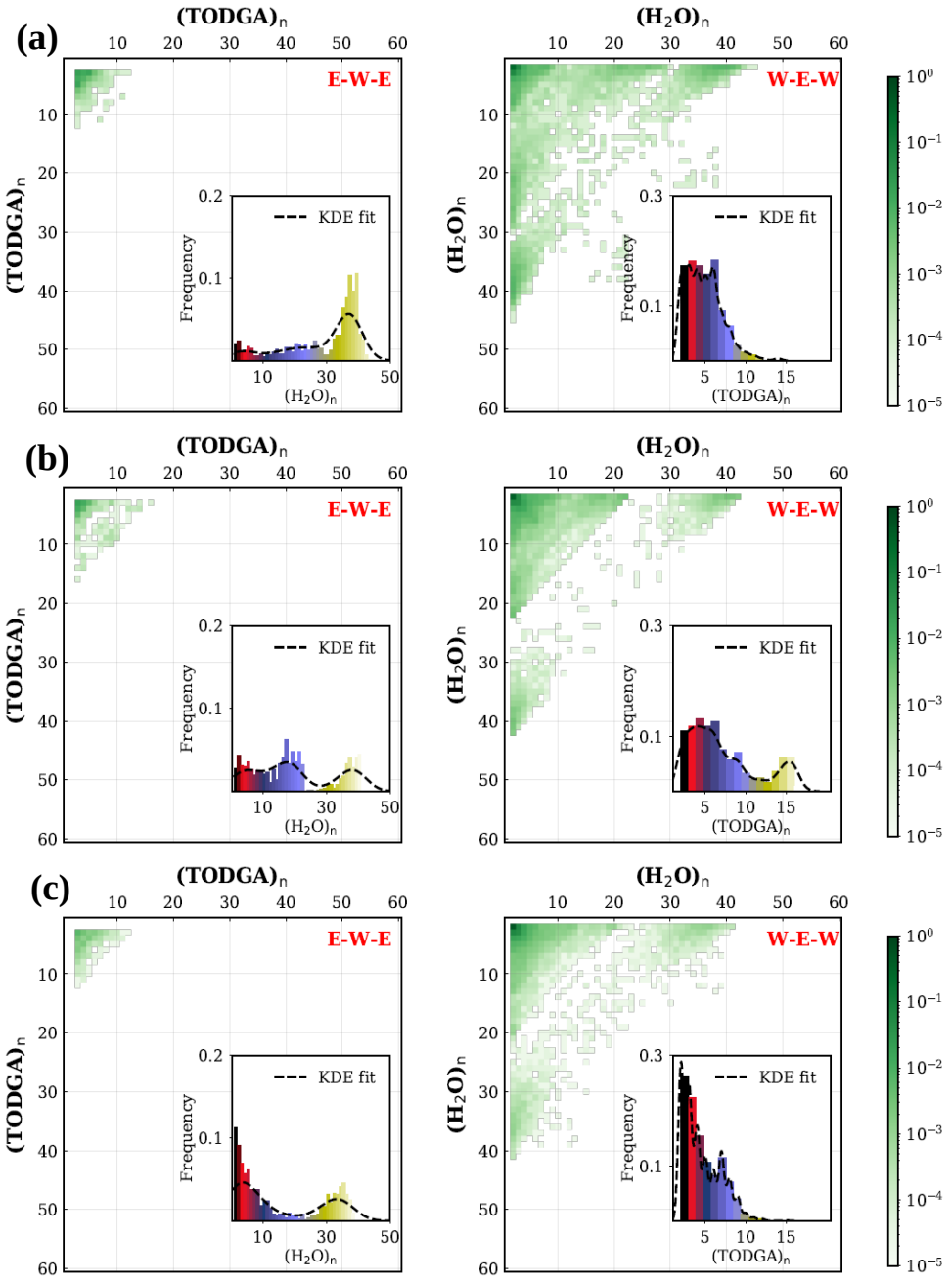

Figure 4: The plot describes the growth of bridged assemblies between water and TODGA for C3 (top), C4 (middle) and C5 (bottom) systems. Left panel represents occurrences of Extractant-Water-Extractant (E-W-E) mixed-aggregates where water bridges the TODGA clusters. Right panel represents occurrences of Water-Extractant-Water (W-E-W) mixed-aggregates where TODGA bridges the water clusters. The color bar is in logarithmic scale and indicate the normalized proportion of the total occurrences of E-W-E and W-E-W mixed-aggregates as function of the cluster sizes of bridged entities. The inset box within the plots shows the normalized frequency distribution of occurrences (Y axis) of the bridging constituents (left panel: water; right panel: TODGA) with respect to their cluster size (X axis).The shape of the distribution in the inset box is obtained using gaussian kernel density estimate (KDE).

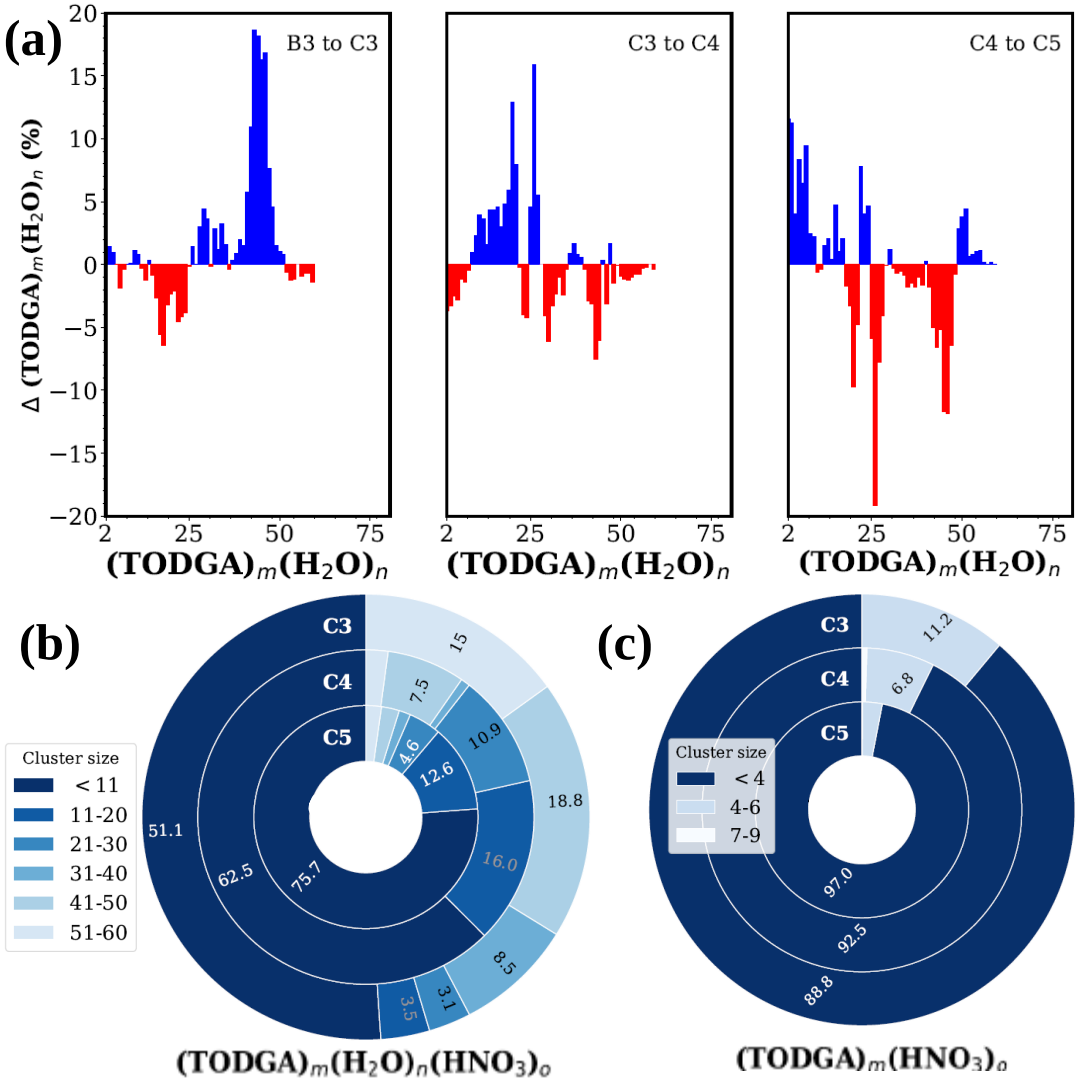

Figure 5: (a) The relative change in the percentage of $(TODGA)_m(H_2O)_n$ mixed-aggregates progressively from B3 to C3, C4 and C5 systems are plotted against the cluster size (m+n). Radial bar chart on cluster distribution of (b) $(TODGA)_m(H_2O)_n(HNO_3)_o$ and (c) $(TODGA)_m(HNO_3)_o$ mixed aggregates under C3, C4 and C5 condition (values on the chart indicates % of clusters within respective size interval (only values >3 % are shown for clarity).

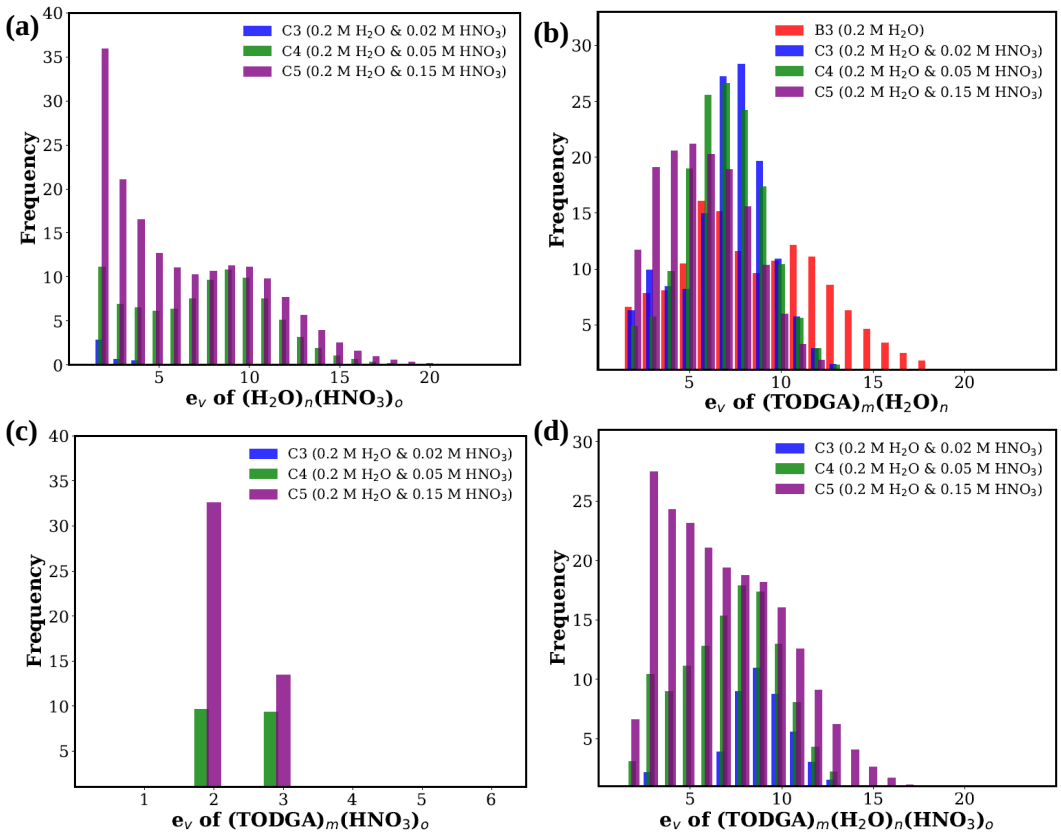

Figure 6: Distribution of eccentricities (e_v) associated with (a) Water-Nitric acid network, (b) TODGA-Water network, (c) TODGA-Nitric acid (d) TODGA-Water-Nitric acid network under C3, C4 and C5 conditions. Frequency quantifies the total number of instances of e_v for all the molecules of associated mixed-aggregates type.

4. Conclusion

Molecular simulation combined with detailed hydrogen bond network analysis predict that polar co-solutes impact the size and shape of self-assembled amphiphile extractants in a manner consistent with the competition of energetic contributions from different types of hydrogen bonding (i.e., between the polar solutes with the amphiphile, between solutes of the same and different types). Necessarily, this is a concentration dependent phenomenon and is sensitive to the number of hydrogen bond donor and acceptor sites on the co-solutes.

Using a well-known liquid-liquid extraction system as a test case, we originally hypothesized that the self-assembly of a representative diglycolomide extractant (TODGA) would differ based upon the hydrogen bond properties of co-extracted H_2O and HNO_3, as has been observed in analogous aqueous studies of amphiphile self-assembly[17, 16]. Yet graph theoretical and clustering analysis of the network of intermolecular interactions reveals a surprising breadth of the affect of hydrogen bonding, and more importantly competition of those interactions, upon amphiphile aggregation. Consider that at low water concentration in the organic phase, individual H_2O molecules support TODGA self-assembly through local bridging hydrogen bond interactions. Yet as $[H_2O]_{org}$ increases, $H_2O...H_2O$ hydrogen bonding and self-solvation drives the formation of large $(H_2O)_n$ clusters that shift the TODGA self-assembly paradigm into an extended aggregation framework - based upon TODGA clusters adsorbed to the periphery of $(H_2O)_n$. There is thus concentration dependent competition of H_2O hydrogen bonding with TODGA (which is favored at low $[H_2O]_{org}$) and $H_2O...H_2O$ hydrogen bonding (which is favored at high $[H_2O]_{org}$).

The introduction of a competing hydrogen bonding co-solute, in this case HNO_3 which is co-extracted with H_2O in LLE systems, introduces an additional degree of freedom as it pertains to the hydrogen bonding network that drives TODGA self-assembly pathways. The large number of accepting hydrogen bond sites in HNO_3 out-compete $H_2O...H_2O$ hydrogen bonding. As such, when nitric acid is introduced into the organic solution it prevents the formation of large $(H_2O)_n$ and thus limits the formation of extended TODGA aggregation. Nitric acid can thus be considered a solute that fosters the growth of small and medium-sized amphiphile assemblies with a composition of TODGA-H_2O-HNO_3 as $[HNO_3]_{org}$ increases.

The presence of water and acid in non-polar media is experimentally well-

known to enhance self-assembly of amphiphiles extractants in LLE systems.[22, 19, 13, 26, 27] Yet the coextraction of these solutes has prevented rigorous control over their organic phase concentration[20, 18, 19, 22] and thus prevented mechanistic insight. Broadly implicit within the literature is the supposition that HNO_3 rather than H_2O is responsible for enhanced extractant aggregation, although a synergistic effect has also been attributed. Instead, this work provides evidence for self-assembly that is driven by intense competition between different hydrogen bond environments, where concentration of those environments plays a key role. Within conditions related to LLE we propose that water as a polar co-solute is the primary driving force behind extractant aggregation. This work forms the basis for a fundamental understanding of how varying hydrogen bond characteristics and solvation properties influence self-assembly of amphiphiles in non-polar media. Further, as it pertains to LLE, the results from this work will help within the experimental design of separations systems that can tune aggregation behavior to influence separations efficiency.

CRediT authorship contribution statement

Biswajit Sadhu: Methodology, Conceptualization, Investigation, Formal analysis, Writing – original draft, Writing – review & editing. **Aurora E. Clark:** Funding acquisition, Project administration, Supervision, Conceptualization, Writing – review & editing.

Declaration of Competing Interest

The authors declare that they have no known competing financial interests or personal relationships that could have influence the present work.

Acknowledgement

This work was supported by the U.S. Department of Energy (DOE), Basic Energy Sciences, Chemical Sciences, Geosciences, and Biosciences Division under contract DEAC02-06CH11357. This research used resources from the Center for Institutional Research Computing at Washington State University. B.S. thanks Bhabha Atomic Research Centre (BARC), Mumbai, India for granting extra-ordinary leave to work at Washington State University.

Appendix A. Supplementary data

Simulation snapshots, cluster analysis details under **C1** and **C2** conditions, cluster analysis results for studied systems, extended aggregation between water and acid molecules, short-range non-bonded interaction energy vs. simulation time plots, oxygen-oxygen RDF profiles of water molecules.

References

[1] F. Herbst, K. Schrœter, I. Gunkel, S. Grœger, T. Thurn-Albrecht, J. Balbach, W. H. Binder, Aggregation and chain dynamics in supramolecular polymers by dynamic rheology: cluster formation and self-aggregation, Macromolecules 43 (23) (2010) 10006–10016.

[2] S. Park, J.-H. Lim, S.-W. Chung, C. A. Mirkin, Self-assembly of mesoscopic metal-polymer amphiphiles, Science 303 (5656) (2004) 348–351.

[3] B. Charleux, G. Delaittre, J. Rieger, F. D'Agosto, Polymerization-induced self-assembly: from soluble macromolecules to block copolymer nano-objects in one step, Macromolecules 45 (17) (2012) 6753–6765.

[4] C. Le Bon, T. Nicolai, D. Durand, Kinetics of aggregation and gelation of globular proteins after heat-induced denaturation, Macromolecules 32 (19) (1999) 6120–6127.

[5] Y. M. Yamada, S. M. Sarkar, Y. Uozumi, Amphiphilic self-assembled polymeric copper catalyst to parts per million levels: click chemistry, J. Am. Chem. Soc. 134 (22) (2012) 9285–9290.

[6] C. Efthymiou, L. M. Bergström, J. N. Pedersen, J. S. Pedersen, P. Hansson, Self-assembling properties of ionisable amphiphilic drugs in aqueous solution, Journal of Colloid and Interface Science 600 (2021) 701–710.

[7] A. Rösler, G. W. Vandermeulen, H.-A. Klok, Advanced drug delivery devices via self-assembly of amphiphilic block copolymers, Adv. Drug Deliv. Rev. 64 (2012) 270–279.

[8] X.-F. Xu, C.-Y. Pan, W.-J. Zhang, C.-Y. Hong, Polymerization-induced self-assembly generating vesicles with adjustable ph-responsive release performance, Macromolecules 52 (5) (2019) 1965–1975.

[9] A. Ianiro, H. Wu, M. M. van Rijt, M. P. Vena, A. D. Keizer, A. C. C. Esteves, R. Tuinier, H. Friedrich, N. A. Sommerdijk, J. P. Patterson, Liquid–liquid phase separation during amphiphilic self-assembly, Nat. Chem. 11 (4) (2019) 320–328.

[10] M. J. Servis, B. Sadhu, L. Soderholm, A. E. Clark, Amphiphile conformation impacts aggregate morphology and solution structure across multiple lengthscales, Journal of Molecular Liquids 345 (2022) 117743.

[11] T. Zemb, M. Duvail, J.-F. Dufrêche, Reverse aggregates as adaptive self-assembled systems for selective liquid-liquid cation extraction, Isr. J. Chem. 53 (1-2) (2013) 108–112.

[12] K. Rama Swami, K. Venkatesan, M. Antony, Aggregation behavior of alkyldiglycolamides in n-dodecane medium during the extraction of nd (iii) and nitric acid, Ind. Eng. Chem. Res. 57 (40) (2018) 13490–13497.

[13] T. Yaita, A. Herlinger, P. Thiyagarajan, M. Jensen, Influence of extractant aggregation on the extraction of trivalent f-element cations by a tetraalkyldiglycolamide, Solvent Extr. Ion Exch. 22 (4) (2004) 553–571.

[14] M. šspadina, K. Bohinc, T. Zemb, J.-F. Dufrêche, Synergistic solvent extraction is driven by entropy, ACS Nano 13 (12) (2019) 13745–13758.

[15] R. J. Ellis, Y. Meridiano, J. Muller, L. Berthon, P. Guilbaud, N. Zorz, M. R. Antonio, T. Demars, T. Zemb, Complexation-induced supramolecular assembly drives metal-ion extraction, Chem. Eur. J 20 (40) (2014) 12796–12807.

[16] A. Sikder, S. Ghosh, Hydrogen-bonding regulated assembly of molecular and macromolecular amphiphiles, Mater. Chem. Front. 3 (2019) 2602–2616.

[17] S. E. Paramonov, H.-W. Jun, J. D. Hartgerink, Self-assembly of peptideamphiphile nanofibers: the roles of hydrogen bonding and amphiphilic packing, Journal of the American Chemical Society 128 (22) (2006) 7291–7298.

[18] C. Gaillard, V. Mazan, S. Georg, O. Klimchuk, M. Sypula, I. Billard, R. Schurhammer, G. Wipff, Acid extraction to a hydrophobic ionic liquid: the role of added tributylphosphate investigated by experiments and simulations, Phys. Chem. Chem. Phys. 14 (15) (2012) 5187–5199.

[19] K. Naito, T. Suzuki, The mechanism of the extraction of several proton acids by tri-n-butyl phosphate, J. Phys. Chem. 66 (6) (1962) 983–988.

[20] E. L. Campbell, V. E. Holfeltz, G. B. Hall, K. L. Nash, G. J. Lumetta, T. G. Levitskaia, Nitric acid and water extraction by t2ehdga in n-dodecane, Solvent Extr. Ion Exch. 35 (7) (2017) 586–603.

[21] E. S. Shamay, V. Buch, M. Parrinello, G. L. Richmond, At the water's edge: Nitric acid as a weak acid, J. Am. Chem. Soc. 129 (43) (2007) 12910–12911.

[22] J. Jiang, W. Li, H. Gao, J. Wu, Extraction of inorganic acids with neutral phosphorus extractants based on a reverse micelle/microemulsion mechanism, J. Colloid Interface Sci. 268 (1) (2003) 208–214.

[23] S. Ansari, P. Pathak, V. Manchanda, M. Husain, A. Prasad, V. Parmar, N,n,n′,n′-tetraoctyl diglycolamide (todga): a promising extractant for actinide-partitioning from high-level waste (hlw), Solvent Extr. Ion Exch. 23 (4) (2005) 463–479.

[24] P. Pathak, S. Ansari, S. Kumar, B. Tomar, V. Manchanda, Dynamic light scattering study on the aggregation behaviour of n, n, n, n-tetraoctyl diglycolamide (todga) and its correlation with the extraction behaviour of metal ions, J. Colloid Interface Sci. 342 (1) (2010) 114–118.

[25] D. Whittaker, A. Geist, G. Modolo, R. Taylor, M. Sarsfield, A. Wilden, Applications of diglycolamide based solvent extraction processes in spent nuclear fuel reprocessing, part 1: Todga, Solvent Extr. Ion Exch. 36 (3) (2018) 223–256.

[26] S. Nave, G. Modolo, C. Madic, F. Testard, Aggregation properties of n,n,n′,n′-tetraoctyl-3-oxapentanediamide (todga) in n-dodecane, Solvent Extr. Ion Exch. 22 (4) (2004) 527–551.

[27] M. P. Jensen, T. Yaita, R. Chiarizia, Reverse-micelle formation in the partitioning of trivalent f-element cations by biphasic systems containing a tetraalkyldiglycolamide, Langmuir 23 (9) (2007) 4765–4774.

[28] Q. N. Vo, L. X. Dang, M. Nilsson, H. D. Nguyen, Quantifying dimer and trimer formation by tri-n-butyl phosphates in n-dodecane: Molecular dynamics simulations, J. Phys. Chem. B 120 (28) (2016) 6985–6994.

[29] J. Wang, R. M. Wolf, J. W. Caldwell, P. A. Kollman, D. A. Case, Development and testing of a general amber force field, J. Comput. Chem 25 (9) (2004) 1157–1174.

[30] A. D. Becke, Density-functional thermochemistry. i. the effect of the exchange-only gradient correction, J. Chem. Phys. 96 (3) (1992) 2155–2160.

[31] C. Lee, W. Yang, R. G. Parr, Development of the colle-salvetti correlation-energy formula into a functional of the electron density, Phys. Rev. B 37 (2) (1988) 785.

[32] W. J. Hehre, R. Ditchfield, J. A. Pople, Self—consistent molecular orbital methods. xii. further extensions of gaussian—type basis sets for use in molecular orbital studies of organic molecules, J. Chem. Phys. 56 (5) (1972) 2257–2261.

[33] M. Hirata, P. Guilbaud, M. Dobler, S. Tachimori, Molecular dynamics simulations for the complexation of ln^{3+} and $uo_2{}^{2+}$ ions with tridentate ligand diglycolamide (dga), Phys. Chem. Chem. Phys. 5 (4) (2003) 691–695.

[34] S. Ansari, P. Mohapatra, D. Prabhu, V. Manchanda, Evaluation of n, n, n′, n′-tetraoctyl-3-oxapentane-diamide (todga) as a mobile carrier in remediation of nuclear waste using supported liquid membrane, J. Membr. Sci. 298 (1-2) (2007) 169–174.

[35] R. Ganguly, J. N. Sharma, N. Choudhury, Todga based w/o microemulsion in dodecane: An insight into the micellar aggregation characteristics by dynamic light scattering and viscometry, J. Colloid Interface Sci. 355 (2) (2011) 458–463.

[36] W. L. Jorgensen, C. Jenson, Temperature dependence of tip3p, spc, and tip4p water from npt monte carlo simulations: Seeking temperatures of maximum density, J. Comput. Chem 19 (10) (1998) 1179–1186.

[37] Q. N. Vo, L. X. Dang, H. D. Nguyen, M. Nilsson, Microscopic behaviors of tri-n-butyl phosphate, n-dodecane, and their mixtures at air/liquid and liquid/liquid interfaces: An amber polarizable force field study, The Journal of Physical Chemistry B 123 (3) (2019) 655–665.

[38] M. J. Servis, D. T. Wu, J. C. Braley, Network analysis and percolation transition in hydrogen bonded clusters: nitric acid and water extracted by tributyl phosphate, Phys. Chem. Chem. Phys. 19 (18) (2017) 11326–11339.

[39] M. H. Kuo, A. David, N. Kamelamela, M. White, M. J. Shultz, Nitric acid- water interaction probed via isolation in carbon tetrachloride, J. Phys. Chem. C 111 (25) (2007) 8827–8831.

[40] Y. Miller, R. B. Gerber, Dynamics of proton recombination with no_3^- anion in water clusters, Phys. Chem. Chem. Phys. 10 (8) (2008) 1091–1093.

[41] L. Martínez, R. Andrade, E. G. Birgin, J. M. Martínez, Packmol: a package for building initial configurations for molecular dynamics simulations, J. Comput. Chem 30 (13) (2009) 2157–2164.

[42] M. J. Abraham, T. Murtola, R. Schulz, S. Páll, J. C. Smith, B. Hess, E. Lindahl, Gromacs: High performance molecular simulations through multi-level parallelism from laptops to supercomputers, SoftwareX 1 (2015) 19–25.

[43] H. J. Berendsen, J. v. Postma, W. F. van Gunsteren, A. DiNola, J. R. Haak, Molecular dynamics with coupling to an external bath, J. Chem. Phys. 81 (8) (1984) 3684–3690.

[44] D. J. Evans, B. L. Holian, The nose–hoover thermostat, J. Chem. Phys. 83 (8) (1985) 4069–4074.

[45] U. Essmann, L. Perera, M. L. Berkowitz, T. Darden, H. Lee, L. G. Pedersen, A smooth particle mesh ewald method, J. Chem. Phys. 103 (19) 8577–8593.

[46] B. Hess, H. Bekker, H. J. Berendsen, J. G. Fraaije, Lincs: a linear constraint solver for molecular simulations, J. Comput. Chem 18 (12) (1997) 1463–1472.

[47] A. Ozkanlar, A. E. Clark, Chemnetworks: a complex network analysis tool for chemical systems, J. Comput. Chem 35 (6) (2014) 495–505.

[48] A. Hagberg, P. Swart, D. S Chult, Exploring network structure, dynamics, and function using networkx, Tech. rep., Los Alamos National Lab.(LANL), Los Alamos, NM (United States) (2008).

[49] K. Han, R. M. Venable, A.-M. Bryant, C. J. Legacy, R. Shen, H. Li, B. Roux, A. Gericke, R. W. Pastor, Graph–theoretic analysis of monomethyl phosphate clustering in ionic solutions, J. Phys. Chem. B 122 (4) (2018) 1484–1494.

[50] M. Velinova, D. Sengupta, A. V. Tadjer, S.-J. Marrink, Sphere-to-rod transitions of nonionic surfactant micelles in aqueous solution modeled by molecular dynamics simulations, Langmuir 27 (23) (2011) 14071–14077.

[51] A. Ozkanlar, T. Zhou, A. E. Clark, Towards a unified description of the hydrogen bond network of liquid water: A dynamics based approach, J. Chem. Phys. 141 (21) (2014) 214107.

[52] F. W. Takes, W. A. Kosters, Computing the eccentricity distribution of large graphs, Algorithms 6 (1) (2013) 100–118.

[53] N. Michaud-Agrawal, E. J. Denning, T. B. Woolf, O. Beckstein, Mdanalysis: a toolkit for the analysis of molecular dynamics simulations, J. Comput. Chem 32 (10) (2011) 2319–2327.

[54] C. Erlinger, D. Gazeau, T. Zemb, C. Madic, L. Lefrancois, M. Hebrant, C. Tondre, Effect of nitric acid extraction on phase behavior, microstructure and interactions between primary aggregates in the system dimethyldibutyltetradecylmalonamide (dmdbtdma)/n-dodecane/water: A phase analysis and small angle x-ray scattering (saxs) characterisation study, Solvent Extr. Ion Exch. 16 (3) (1998) 707–738.